Inorg. Chem. **2004**, *43*, 2932–2942

Variable π-Bonding in Iron(II) Porphyrinates with Nitrite, CO, and *tert*-Butyl Isocyanide: Characterization of $[Fe(TpivPP)(NO_2)(CO)]^-$

Habib Nasri,[†] Mary K. Ellison,[‡] Maoyu Shang,[‡] Charles E. Schulz,*[,§] and W. Robert Scheidt*[,‡]

Department of Chemistry and Biochemistry, University of Notre Dame, Notre Dame, Indiana 46556, Faculté des Sciences de Monastir, Avenue de l'environnement, 5019 Monastir, Tunisia, and Department of Physics, Knox College, Galesburg, Illinois 61401

Received September 23, 2003

The addition of the strongly π-bonding ligands CO or *tert*-butyl isocyanide to the low-spin five-coordinate iron(II) nitrite species $[Fe(TpivPP)(NO_2)]^-$ (TpivPP = picket fence porphyrin) gives two new six-coordinate species $[Fe(TpivPP)(NO_2)(CO)]^-$ and $[Fe(TpivPP)(NO_2)(t\text{-BuNC})]^-$. These species have been characterized by single-crystal structure determinations and by UV–vis, IR, and Mössbauer spectroscopies. All evidence shows that in the mixed-ligand iron(II) porphyrin species, $[Fe(TpivPP)(NO_2)(CO)]^-$, the two trans, π-accepting ligands CO and nitrite compete for π density. The CO ligand however dominates the bonding. The Fe–N(NO_2) bond lengths for the two independent anions in the unit cell at 2.006(4) and 2.009(4) Å are lengthened compared to other nitrite species with either no trans ligands or non-π-accepting trans ligands to nitrite. The Fe–C(CO) bond lengths are 1.782(4) Å and 1.789(5) Å for the two anions. The two Fe–C–O angles at 175.5(4) and 177.5(4)° are essentially linear in both anions. The quadrupole splitting for $[Fe(TpivPP)(NO_2)(CO)]^-$ was determined to be 0.32 mm/s, and the isomer shift was 0.18 mm/s at room temperature in zero applied field. Both of the Mössbauer parameters are much smaller than those found for six-coordinate low-spin iron(II) porphyrinates with neutral nitrogen-donating ligands as well as iron(II) nitro complexes. However, the Mössbauer parameters are typical of other six-coordinate CO porphyrinates signifying that CO is the more dominant ligand. The CO stretching frequency of 1974 cm^{-1} is shifted only slightly to higher energy compared to six-coordinate CO complexes with neutral nitrogen-donor ligands trans to CO. Crystal data for $[K(222)][Fe(TpivPP)(NO_2)(CO)]\cdot 1/2C_6H_5Cl$: monoclinic, space group $P2_1/c$, $Z = 8$, $a = 33.548(6)$ Å, $b = 18.8172(15)$ Å, $c = 27.187(2)$ Å, $\beta = 95.240(7)°$, $V = 17091(4)$ Å^3.

Introduction

The binding of the diatomic molecules O_2, CO, and NO to heme proteins is extremely important to mammalian physiology, while the binding of nitric oxide (NO), nitrite (NO_2^-), and nitrate (NO_3^-) to hemes is involved in important denitrification processes. Hence, the study of the bonding interaction between these biologically significant small molecules and others to hemes has been and continues to be an active area of research.[1−3] However, despite great advances in understanding the many biological functions of these molecules, there remains considerable controversy about the mechanisms and identities of possible intermediates involved in their numerous reactions. For instance, the discrimination in binding of O_2 over CO to hemes in respiration is not completely understood.[4,5] In addition, it is proposed that many of the intermediates in the inorganic nitrogen cycle involve the interaction of hemes with small nitrogen containing molecules; the exact identities of several are only speculative. In a recent mechanistic study[6] of the reduction of nitrite to ammonia by cytochrome *c* nitrite

* Authors to whom correspondence should be addressed. E-mail: W.R.Scheidt.1@nd.edu (W.R.S.).
† Faculté des Sciences de Monastir.
‡ University of Notre Dame.
§ Knox College.

(1) Wyllie, G. R. A.; Scheidt, W. R. *Chem. Rev.* **2002**, *102*, 1067.
(2) Averill, B. A. *Chem. Rev.* **1996**, *96*, 2951.
(3) Scheidt, W. R.; Ellison, M. K. *Acc. Chem. Res.* **1999**, *32*, 350.
(4) A *JBIC* commentary has appeared: *JBIC, J. Biol. Inorg. Chem.* **1997**, *2*, 515−552. The parts are as follows: (a) Spiro, T. G.; Kozlowski, P. M. *JBIC, J. Biol. Inorg. Chem.* **1997**, *2*, 516. (b) Slebodnick, C.; Ibers, J. A. *JBIC, J. Biol. Inorg. Chem.* **1997**, *2*, 521. (c) Vangberg, T.; Bocian, D. F.; Ghosh, A. *JBIC, J. Biol. Inorg. Chem.* **1997**, *2*, 526. (d) Lim, M.; Jackson, T. A.; Anfinrud, P. A. *JBIC, J. Biol. Inorg. Chem.* **1997**, *2*, 531. (e) Sage, J. T. *JBIC, J. Biol. Inorg. Chem.* **1997**, *2*, 537. (f) Olson, J. S.; Phillips, G. N., Jr. *JBIC, J. Biol. Inorg. Chem.* **1997**, *2*, 544.
(5) Kachalova, G. S.; Popov, A. N.; Bartunik, H. D. *Science (Washington, D.C.)* **1999**, *284*, 473.

10.1021/ic035119y CCC: $27.50
Published on Web 04/06/2004

reductase (ccNiR), it was proposed that the binding of nitrite to an iron(II) heme which starts the reaction cycle depends on the strong π bond between nitrite and iron(II). The π bond leads to a strong Fe−N bond and a weakened N−O bond which can be cleaved heterolytically. Hence, the nature of the bond between nitrite and iron is critically important to the activation of this enzyme. Clearly, gaining insight into the bonding interaction between these small molecules and hemes through structural and physical studies is of interest.

Structural studies on heme proteins with CO as an axial ligand report a wide range of angles for the Fe−C−O group.[5−9] This description of the Fe−C−O geometry is less than satisfactory when trying to observe small distortions in the metal−ligand bonding due to changes in the ligand environment. Consequently, model metalloporphyrin compounds have been used to more precisely define the metal−ligand geometries. A number of six-coordinate (carbonyl)-iron(II) porphyrin derivatives have been structurally characterized.[10−19] In all cases, the Fe−C−O angle is essentially linear (Fe−C−O > 175°).

Over the years, our laboratory has synthesized and characterized a number of iron(II)[20−22] and iron(III)[23−26] porphyrin complexes where NO_2^- is an axial ligand. The structural and electronic characterization of these (nitro)iron porphyrin derivatives has shown that the bonding interaction between iron and the anionic nitrite ligand is quite variable. For instance, nitrite acts as a strong π-acceptor ligand in the five-coordinate low-spin iron(II) species $[Fe(TpivPP)(NO_2)]^-$.[20,22,27] Addition of the neutral ligands pyridine or pentamethylene sulfide to give the six-coordinate species $[Fe(TpivPP)(NO_2)(Py)]^-$ and $[Fe(TpivPP)(NO_2)(PMS)]^-$ significantly reduces the π-bonding ability of nitrite as shown by single-crystal structure determinations and Mössbauer spectroscopy.[22]

We have also characterized two forms of the mixed-ligand, six-coordinate iron(II) species $[Fe(TpivPP)(NO_2)(NO)]^-$.[21] The main difference in the two forms is that the plane defined by the axial ligand NO_2^- and the nitrosyl Fe−N−O plane has either relative perpendicular or parallel orientation. These different ligand orientations have an effect on the electronic structure at iron as shown by Mössbauer spectroscopy. The form with relative perpendicular ligand planes maximizes the π bonding while in the parallel form the two coplanar ligands are competing for π density.

In further attempts to systematically study the bonding variability of the anionic nitrite ligand, we now report the syntheses and characterization of two new mixed-ligand, six-coordinate iron(II) porphyrin complexes where the ligands CO or *tert*-butylisocyanide are trans to nitrite. The syntheses involve adding the new sixth ligand to the five-coordinate iron(II) species $[Fe(TpivPP)(NO_2)]^-$. Picket fence porphyrin is used to protect the reactive nitrite group.[28] Mössbauer data show that, in the complex $[Fe(TpivPP)(NO_2)(CO)]^-$, the presence of the strong π-accepting carbonyl ligand is quite effective at reducing the π interaction between iron and nitrite. In addition, structural data show that the presence of the nitrite ligand trans to CO does not lead to significant distortion of the FeCO group compared to previously characterized species with neutral nitrogen-donor ligands trans to CO.

Experimental Section

General Information. All manipulations for the preparation of the iron(II) six-coordinate porphyrin derivatives (see below) were carried out under argon using a double-manifold vacuum line, Schlenkware, and cannula techniques. Chlorobenzene was purified by washing with concentrated sulfuric acid and then with water until the aqueous layer was neutral, then dried with $MgSO_4$, and then distilled twice over P_2O_5.[29] Hexanes were distilled from

(6) Einsle, O.; Messerschmidt, A.; Huber, R.; Kroneck, P. M. H.; Neese, F. *J. Am. Chem. Soc.* **2002**, *124*, 11737.
(7) Quillin, M. L.; Arduini, R. M.; Olson, J. S.; Phillips, G. N., Jr. *J. Mol. Biol.* **1993**, *234*, 140.
(8) Kuriyan, J.; Wilz, S.; Karplus, M.; Petsko, G. A. *J. Mol. Biol.* **1986**, *192*, 133.
(9) Vojtěchivský, J.; Chu, K.; Berendzen, J.; Sweet, R. M.; Schlicting, I. *Biophys. J.* **1999**, 2153.
(10) Peng, S.-M.; Ibers, J. A. *J. Am. Chem. Soc.* **1976**, *98*, 8032.
(11) Salzmann, R.; Ziegler, C. J.; Godbout, N.; McMahon, M. T.; Suslick, K. S.; Oldfield, E. *J. Am. Chem. Soc.* **1998**, *120*, 11323.
(12) Salzmann, R.; McMahon, M. T.; Godbout, N.; Sanders, L. K.; Wojdelski, M.; Oldfield, E. *J. Am. Chem. Soc.* **1999**, *121*, 3818.
(13) Scheidt, W. R.; Haller, K. J.; Fons, M.; Mashiko, T.; Reed, C. A. *Biochemistry* **1981**, *20*, 3653.
(14) Caron, C.; Mitschler, A.; Rivère, G.; Ricard, L.; Schappacher, M.; Weiss, R. *J. Am. Chem. Soc.* **1979**, *101*, 7401.
(15) Ricard, L.; Weiss, R.; Momenteau, M. *J. Chem. Soc., Chem. Commun.* **1986**, 818.
(16) Kim, K.; Fettinger, J.; Sessler, J. L.; Cyr, M.; Hugdahl, J.; Collman, J. P.; Ibers, J. A. *J. Am. Chem. Soc.* **1989**, *111*, 403.
(17) Kim, K.; Ibers, J. A. *J. Am. Chem. Soc.* **1991**, *113*, 6077.
(18) Slebodnick, C.; Duval, M. L.; Ibers, J. A. *Inorg. Chem.* **1996**, *35*, 3607.
(19) Slebodnick, C.; Fettinger, J. C.; Peterson, H. B.; Ibers, J. A. *J. Am. Chem. Soc.* **1996**, *118*, 3216.
(20) Nasri, H.; Wang, Y.; Huynh, B. H.; Scheidt, W. R. *J. Am. Chem. Soc.* **1991**, *113*, 717.
(21) Nasri, H.; Ellison, M. K.; Chen, S.; Huynh, B. H.; Scheidt, W. R. *J. Am. Chem. Soc.* **1997**, *119*, 6274.
(22) Nasri, H.; Ellison, M. K.; Krebs, C.; Huynh, B. H.; Scheidt, W. R. *J. Am. Chem. Soc.* **2000**, *122*, 10795.
(23) Nasri, H.; Goodwin, J. A.; Scheidt, W. R. *Inorg. Chem.* **1990**, *29*, 185.
(24) Nasri, H.; Wang, Y.; Huynh, B. H.; Walker, F. A.; Scheidt, W. R. *Inorg. Chem.* **1991**, *30*, 1483.
(25) Nasri, H.; Haller, K. J.; Wang, Y.; Huynh, B. H.; Scheidt, W. R. *Inorg. Chem.* **1992**, *31*, 3459.
(26) Ellison, M. K.; Schulz, C. E.; Scheidt, W. R. *Inorg. Chem.* **1999**, *38*, 100.

(27) Abbreviations: Porph, a generalized porphyrin dianion; T*p*-OCH_3-PP, dianion of *meso*-tetrakis(*p*-methoxyphenyl)porphyrin; TPP, dianion of *meso*-tetraphenylporphyrin; TMP, *meso*-tetramesitylporphyrin; OEP, dianion of 2,3,7,8,12,13,17,18-octaethylporphyrin; Deut, deuteroporphyrin IX dimethyl ester; TpivPP, dianion of α,α,α,α-tetrakis(*o*-pivalamidophenyl)porphyrin; $TPpiv_2C_{12}P$, dianion of 5,15-[2,2′-(dodecanediamido)diphenyl]-α,α-10,20-bis(*o*-pivaloylaminophenyl)-porphyrin; *β*-PocpivP, dianion of "pocket" porphyrin; C_2-Cap and C_3-Cap, dianion of "capped" porphyrins; OC_3OPor, dianion of "benzene capped" porphyrin; PMS, pentamethylene sulfide; Py, pyridine; THT, tetrahydrothiophene; THF, tetrahydrofuran; HIm, imidazole; 1-MeIm, 1-methylimidazole; 2-MeHIm, 2-methylimidazole; $1,2\text{-}Me_2Im$, 1,2-dimethylimidazole; $4\text{-}NMe_2Py$, 4-*N*-(dimethylamino)pyridine; Pip, piperidine; 4-MePip, 4-methylpiperidine; Pz, pyrazole; 1-VinIm, 1-vinylimidazole; 1-BzlIm, 1-benzylimidazole; 1-AcIm, 1-acetylimidazole; Iz, indazole (benzopyrazole); SC_6HF_4, 2,3,5,6-tetrafluorobenzenethiolate; SPh, benzenethiolate; PMe_3, trimethylphosphine; Kryptofix-222 or 222, 4,7,13,16,21,24-hexaoxo-1,10-diazabicyclo[8.8.8]hexacosane; N_p, porphyrinato nitrogen.

(28) Finnegan, M. G.; Lappin, A. G.; Scheidt, W. R. *Inorg. Chem.* **1990**, *29*, 181.
(29) Armagero, W. L. F.; Perrin, D. D. *Purification of Laboratory Chemicals*, 4th ed.; Butterworth-Heinemann: Woburn, MA, 1997; p 140.

sodium/benzophenone. KNO_2 was recrystallized twice from hot distilled water, dried overnight at about 75 °C, and stored under argon. Kryptofix-222 (Aldrich) was recrystallized from benzene (distilled from sodium/benzophenone) and stored under argon in the dark. The free base (H_2TpivPP) and the corresponding iron(III) chloro and triflato derivatives were synthesized by literature methods.[30,31] UV−vis spectra were recorded on a Perkin-Elmer Lambda 19 UV/vis/near-IR spectrometer, and IR spectra were recorded on a Perkin-Elmer Paragon 10000 FT-IR spectrometer as KBr pellets. Mössbauer measurements were performed on a constant-acceleration spectrometer from 4.2 to 300 K with optional small field and in a 9 T superconducting magnet system (Knox College). A sample of [K(222)][Fe(TpivPP)(NO_2)(CO)]·1/2C_6H_5Cl for Mössbauer spectroscopy was prepared by immobilization of the crystalline material (crystals not ground but washed with water under argon) in Apiezon M grease.

Synthesis of [K(222)][Fe(TpivPP)(NO_2)(CO)]·1/2C_6H_5Cl. [Fe(TpivPP)(SO_3CF_3)(H_2O)] (20 mg, 0.016 mmol) and ∼1 mL of zinc amalgam in 8 mL of chlorobenzene were stirred for about 1 h under argon. The deep red solution of [Fe(TpivPP)] was filtered into a second solution prepared by stirring (overnight) 80 mg of Kryptofix-222 (0.2 mmol) and 185 mg of KNO_2 (2.2 mmol) in 7 mL of chlorobenzene. A stream of CO gas was passed (for about 15 min) through the dark red-yellow solution of the five-coordinate (nitro)iron(II) species, [Fe(TpivPP)(NO_2)]$^-$.[20] The color changes slightly to light red as a result of forming the six-coordinate product [Fe(TpivPP)(NO_2)(CO)]$^-$. Single crystals of this complex were prepared by slow diffusion of hexanes into the chlorobenzene solution. UV−vis in C_6H_5Cl [λ_{max}, nm (log ϵ)]: 414 (sh) (4.67); 434 (5.30); 546 (3.98). IR (KBr): ν(CO) 1974 (m) cm^{-1}; ν(NO_2^-) 1383 (w), 1353 (m) cm^{-1}.

Synthesis of [K(222)][Fe(TpivPP)(NO_2)(*t*-BuNC)]. [Fe(TpivPP)(SO_3CF_3)(H_2O)] (20 mg, 0.016 mmol) and ∼1 mL of zinc amalgam in 8 mL of chlorobenzene were stirred for about 1 h under argon. The deep red solution ([Fe(TpivPP)]) was then filtered into a second solution prepared by stirring (overnight) 80 mg of Kryptofix-222 (0.2 mmol) and 185 mg of KNO_2 (2.2 mmol) in 7 mL of chlorobenzene. To this solution of [Fe(TpivPP)(NO_2)]$^-$ 0.5 mL (4.4 mmol) of *tert*-butyl isocyanide (Aldrich, used without further purification) was added. The color changed to bright-red, and the result of this reaction was the six-coordinate product [Fe(TpivPP)(NO_2)(t-BuNC)]$^-$. X-ray-quality crystals were obtained by liquid diffusion using hexanes as the nonsolvent. UV−vis in C_6H_5Cl [λ_{max}, nm (log ϵ)]: 441 (5.22); 541 (4.20); 572 (3.45). IR (KBr): ν(CN) 2101 (m) cm^{-1}; ν(NO_2^-) 1383 (w), 1345 (m) cm^{-1}.

X-ray Structure Determinations. Single-crystal experiments were carried out on a Nonius FAST area-detector diffractometer at 130 K by methods and procedures for small molecules standard in this laboratory.[32] A brief summary of determined parameters is given in Table 1. The structure was solved in the space group $P2_1/c$ using the direct methods program SHELXS-86.[33] There are two [Fe(TpivPP)(NO_2)(CO)]$^-$ porphyrin anions, two potassium-222 cations, and one molecule of chlorobenzene in the asymmetric unit of structure. One K-cryptand and one porphyrin anion are completely ordered. In the second porphyrin anion, the nitrite ligand and two tertiary butyl groups were found to have two sets of positions caused by rotational disorder. The structure was refined against F^2 with the program SHELXL,[34,35] in which all data collected were used including negative intensities. Complete crystallographic details, atomic coordinates, anisotropic thermal parameters, and fixed hydrogen atom coordinates are included in the Supporting Information. Although the single-crystal structure determination on a sample of [K(222)][Fe(TpivPP)(NO_2)(*t*-BuNC)] clearly showed the identity of both cation and anion including the ligands bound to iron, difficulties in refinement due to substantial disorder led to a structure unsatisfactory for publication.

Table 1. Crystallographic Details for [K(222)][Fe(TpivPP)(NO_2)(CO)]·1/2C_6H_5Cl

formula	$C_{89}H_{105}ClFeKN_{11}O_{13}$
fw	1667.24
a, Å	33.548(6)
b, Å	18.8172(15)
c, Å	27.187(2)
β, deg	95.240(7)
V, Å^3	17 091(4)
Z	8
space group	$P2_1/c$
D_c, g/cm^3	1.296
F(000)	7056
μ, mm^{-1}	0.325
cryst dimens, mm	0.24 × 0.12 × 0.08
abs corr	DIFABS
λ, Å	0.710 73
T, K	130(2)
tot. data collcd	52417
unique data	32 440 (R_{int} = 0.0759)
unique obsd data [$I > 2\sigma(I)$]	21 632
refinement method	on F^2 (SHELXL)
final R indices [$I > 2\sigma(I)$]	R_1 = 0.0775, wR_2 = 0.1850
final R indices (for all data)	R_1 = 0.1224, wR_2 = 0.2200

Results

Reaction of the five-coordinate iron(II) species [Fe(TpivPP)(NO_2)]$^-$ with CO or *tert*-butyl isocyanide gives the new anionic, six-coordinate iron(II) complexes [Fe(TpivPP)(NO_2)(CO)]$^-$ and [Fe(TpivPP)(NO_2)(*t*-BuNC)]$^-$. Care must be taken to eliminate halide impurities that are known to coordinate strongly to iron(II) species. Hence, chlorobenzene was washed with concentrated sulfuric acid and Kryptofix-222 and KNO_2 were recrystallized. The two six-coordinate species were characterized in solution with UV−visible spectroscopy using a specialized inert-atmosphere cell with 1- and 10-mm path lengths. Crystalline anionic iron porphyrinates were obtained as potassium−Kryptofix-222 salts. Both species were characterized by infrared spectroscopy. The carbonyl stretching frequency for [Fe(TpivPP)(NO_2)(CO)]$^-$ appears at 1974 cm^{-1}. The C−N stretch is at 2101 cm^{-1} for [Fe(TpivPP)(NO_2)(*t*-BuNC)]$^-$. The solid-state Mössbauer quadrupole splitting, ΔE_q, for [K(222)][Fe(TpivPP)(NO_2)(CO)]·1/2C_6H_5Cl was found to be 0.32 mm/s, and the isomer shift, δ, was 0.18 mm/s at room temperature in zero applied field.

Single-crystal structure determinations for the two mixed-ligand species unambiguously confirm the presence of the

(30) Collman, J. P.; Gagne, R. R.; Halbert, T. R.; Lang, G.; Robinson, W. T. *J. Am. Chem. Soc.* **1975**, *97*, 1427.
(31) Gismelseed; A.; Bominaar, E. L.; Bill, E.; Trautwein, A. X.; Winkler, H.; Nasri, H.; Doppelt, P.; Mandon, D.; Fischer, J.: Weiss, R. *Inorg. Chem.* **1990**, *29*, 2741.
(32) Scheidt, W. R.; Turowska-Tyrk, I. *Inorg. Chem.* **1994**, *33*, 1314.
(33) Sheldrick, G. M. *Acta Crystallogr.* **1990**, *A46*, 467.
(34) Sheldrick, G. M. *J. Appl. Crystallogr.*, manuscript in preparation.
(35) $R_1 = \Sigma||F_o| - |F_c||/\Sigma|F_o|$ and $wR_2 = \{\Sigma[w(F_o^2 - F_c^2)^2]/\Sigma[wF_o^4]\}^{1/2}$. The conventional R-factors R_1 are based on *F*, with *F* set to zero for negative F^2. The criterion of $F^2 > 2\sigma(F^2)$ was used only for calculating R_1. R-factors based on F^2 (wR_2) are statistically about twice as large as those based on *F*, and R-factors based on *all* data will be even larger.

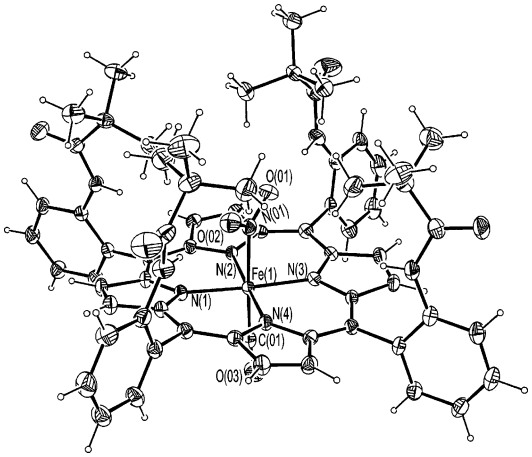

Figure 1. ORTEP diagram of $[Fe(TpivPP)(NO_2)(CO)]^-$ (**1**) showing the coordination at iron. The 50% probability ellipsoids are depicted.

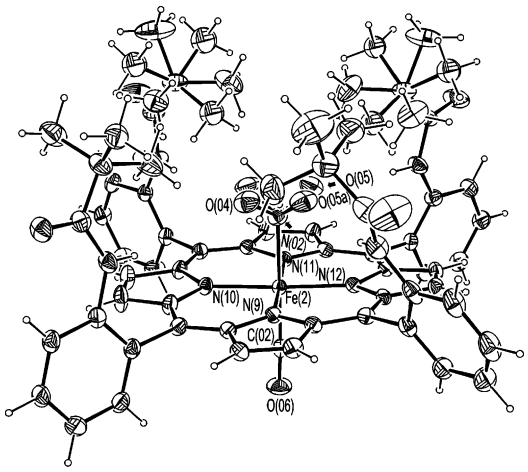

Figure 2. ORTEP diagram of $[Fe(TpivPP)(NO_2)(CO)]^-$ (**2**). The 50% probability ellipsoids are depicted. The rotational disorder in the nitro group and the pivalamide groups are shown.

trans ligands and the K-222 counterions. The detailed structure of [K(222)][Fe(TpivPP)(NO_2)(*t*-BuNC)] will not be reported herein because significant disorder led to difficulties in refinement of the structure. The full formula for the carbonyl derivative is [K(222)][Fe(TpivPP)(NO_2)(CO)]·1/2C_6H_5Cl. This species crystallized in the monoclinic space group $P2_1/c$ with $Z = 8$. There are thus two independent porphyrin anions in the unit cell which are denoted $[Fe(TpivPP)(NO_2)(CO)]^-$ (**1**) and $[Fe(TpivPP)(NO_2)(CO)]^-$ (**2**) or more simply anion **1** and anion **2**. The negative charges are balanced by two independent K-222 counterions, and there is one molecule of chlorobenzene in the asymmetric unit. Figures 1 and 2 are ORTEP diagrams of $[Fe(TpivPP)(NO_2)(CO)]^-$ (**1**) and $[Fe(TpivPP)(NO_2)(CO)]^-$ (**2**), respectively. The complete labeling scheme given in the Supporting Information is consistent with all of the diagrams and tables. In both anions, the nitrite is N-bound and is located inside the protective pocket of the picket fence porphyrin pivalamide groups. The three-atom plane of the nitrite ligands bisect N_p-Fe-N_p angles. The methyl groups of the pivalamide linkages buttress the nitro ligand in anion **1** as can be seen from the view looking down onto the porphyrin plane (Figure 3). The view of anion **2** shown from the nitrite side

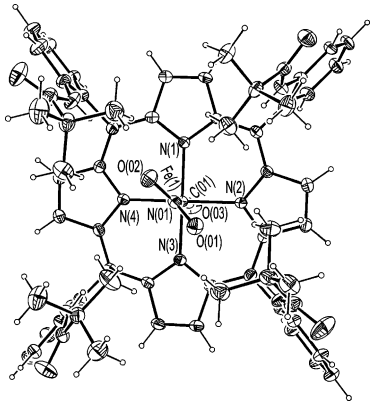

Figure 3. ORTEP diagram of $[Fe(TpivPP)(NO_2)(CO)]^-$ (**1**) looking down on the porphyrin plane.

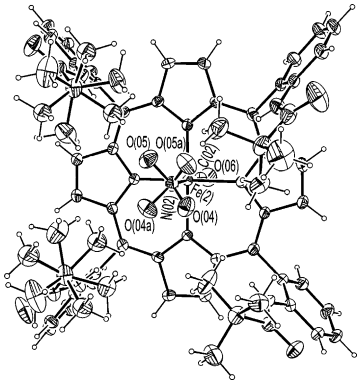

Figure 4. ORTEP diagram of $[Fe(TpivPP)(NO_2)(CO)]^-$ (**2**) looking down on the porphyrin plane.

of the porphyrin plane (Figure 4) clearly depicts the rotational disorder in the nitrite ligand and the methyl groups of two pivalamide arms.

The average equatorial $Fe-N_p$ bond distance is 1.992(7) Å for $[Fe(TpivPP)(NO_2)(CO)]^-$ (**1**) and 1.997(6) Å for $[Fe(TpivPP)(NO_2)(CO)]^-$ (**2**). The $Fe-N(NO_2)$ bond length is 2.006(4) Å for anion **1** and 2.009(4) Å for anion **2**. The Fe−C(CO) bond lengths are 1.782(4) Å and 1.789(5) Å for anion **1** and anion **2**, respectively. The Fe−C−O angles at 175.5(4)° (anion **1**) and 177.5(4)° (anion **2**) are essentially linear in both anions. Complete listings of the bond lengths and angles for both anions, the counterions, and solvent molecule are given in the Supporting Information. Figure 5 gives the formal diagrams for the porphyrinato cores for $[Fe(TpivPP)(NO_2)(CO)]^-$ (**1**) (top) and $[Fe(TpivPP)(NO_2)(CO)]^-$ (**2**) (bottom). The view of the porphyrin is from the nitrite (picket) side of the porphyrin plane. The displacement of each atom from the mean plane of the 24-atom core is displayed (in units of 0.01 Å). Positive displacements are toward the nitrite ligand in each case. The averaged values of each type of bond distance and angle of the core are also given. In each anion, the iron atom is displaced toward the CO ligand. The porphyrin core in anion **1** is modestly ruffled. Dominant ruffled cores are the most common distortion in the iron(II) five- and six-coordinate nitro complexes structurally characterized. Oddly, the direction of the ruffling (the relative ± displacement of the meso carbons with respect to an axial ligand plane) is not dependent on the orientation of

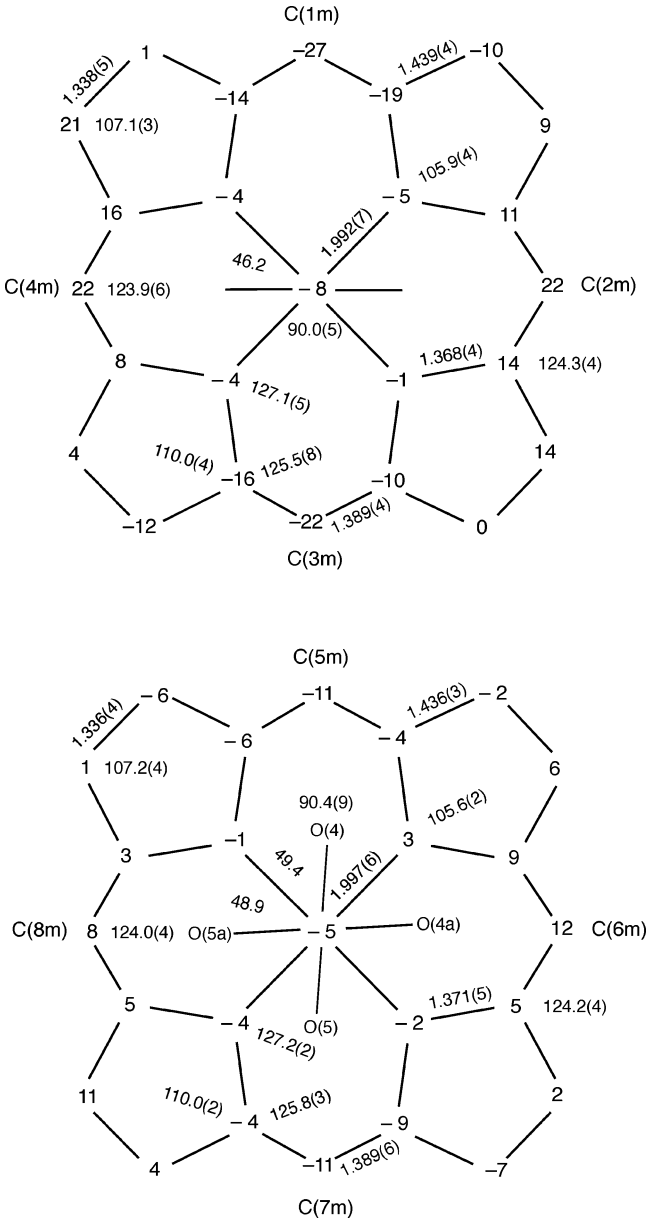

Figure 5. Formal diagrams of the porphyrinato cores of [Fe(TpivPP)(NO$_2$)(CO)]$^-$ (**1**) (top) and [Fe(TpivPP)(NO$_2$)(CO)]$^-$ (**2**) (bottom). Illustrated are the displacements of each atom from the mean plane of the 24-atom porphyrin cores in units of 0.01 Å. Positive values of displacement are toward the NO$_2$ ligand in each anion. The major orientation (54%) of the nitrite in anion **2** is the horizontal orientation. The diagram also gives the averaged values of each distinct bond distance and angle in the porphyrinato cores.

the nitrite ligand. For instance, in [Fe(TpivPP)(NO$_2$)]$^-$,[22] [Fe(TpivPP)(NO$_2$)(NO)]$^-$ (the form with perpendicular axial ligand planes[21]), and [Fe(TpivPP)(NO$_2$)(CO)]$^-$ (**1**), the meso carbon atoms roughly in line with the nitrite ligand plane are actually displaced toward the nitrite side of the porphyrin plane. Figure 5(top) shows this clearly. The carbon atoms C(2m) and C(4m) have a displacement the same sign (+) as the nitrite ligand.

Imposed upon the ruffling is a slight doming of the 4-nitrogen plane toward the CO ligand. Also shown in Figure 5 are the orientations of the nitrite ligand with respect to the porphyrinato nitrogen atoms. In anion **1**, the nitrite plane nearly bisects an N$_p$−Fe−N$_p$ angle (angle is 46.2°). The two orientations of the nitrite ligand are shown for anion **2** (angles are 48.9 and 49.4 °); the occupancies are 54 and 46%. The ruffling of the core in anion **2** is diminished compared to anion **1**.

The charge balance for the two anions is accomplished by two independent Kryptofix-222 counterions. ORTEP diagrams of both cations are given in the Supporting Information. The potassium ion in each case is bound to six oxygen atoms and two nitrogen atoms. The average K−O(222) distance of the two counterions is 2.82(3) Å. The average K−N(222) distance is 3.00(4) Å. Complete listings of the bond lengths and angles are given in the Supporting Information.

Discussion

Over the past several years, we have synthesized a number of (nitro)iron(II) porphyrin species. The successful syntheses of these complexes results from the strategic use of picket fence porphyrin and cryptate (or macrocyclic crown ether) cations. The five-coordinate anionic iron(II) nitrite species [Fe(TpivPP)(NO$_2$)]$^-$ is prepared by addition of cryptand-solubilized KNO$_2$ to the highly air-sensitive four-coordinate species [Fe(TpivPP)]. All of the characterized six-coordinate (nitro)iron(II) species result from the anaerobic addition of gaseous NO or CO or by addition of excess neutral ligand such as pyridine, pentamethylene sulfide, or *tert*-butyl isocyanide to [Fe(TpivPP)(NO$_2$)]$^-$ in solution. As shown by electronic spectroscopy, all of these six-coordinate species persist in solution under anaerobic conditions. In fact, the spectroscopic characterization of [Fe(TpivPP)(NO$_2$)]$^-$ and the resulting six-coordinate species [Fe(TpivPP)(NO$_2$)(L)]$^-$ was our first indication that nitrite is a very unusual ligand. We begin our discussion with the effects of the ligands NO$_2^-$ and CO on the electronic spectrum.

The electronic spectrum of [Fe(TpivPP)(NO$_2$)]$^-$ has a Soret band at 444 nm. As can be seen from the electronic spectral data summarized in Table 2, this 444 nm Soret band for low-spin five-coordinate [Fe(TpivPP)(NO$_2$)]$^-$ is strongly red-shifted compared to all of the other five- or six-coordinate iron−nitro species thus far characterized. It is also strongly red-shifted compared to the spectrum of five-coordinate [Fe(TPP)(CO)]. The addition of a neutral ligand such as PMS or pyridine to [Fe(TpivPP)(NO$_2$)]$^-$ causes the Soret band to blue shift by more than 10 nm. A similar blue shift in the Soret occurs upon addition of NO to the five-coordinate nitrite species. The Soret band at 407 nm for the low-spin, five-coordinate species [Fe(TpivPP)(NO)] is very blue shifted compared to [Fe(TpivPP)(NO$_2$)]$^-$. So what shift in the position of the Soret band should one expect when CO is added trans to nitrite? Probably the most well-known porphyrin CO-related spectroscopic change occurs when CO is added to five-coordinate high-spin thiolate hemes. These are the P450-type porphyrin derivatives, so-called because of the intense red-shifted Soret band at ∼450 nm. A small red shift is also seen when a CO ligand is added to the five-coordinate [Fe(TPP)(CO)] species to give [Fe(TPP)(CO)$_2$].

On the other hand, when CO replaces one of the neutral nitrogen donor ligands in a low-spin, six-coordinate [Fe-

Table 2. Electronic Spectral Data for Selected Iron(II) and Iron(III) Tetraarylporphyrins[a]

complex	λ_{max} (nm) Soret region (log ε)		α, β region (log ε)			ref
Five-Coordinate Iron(II)						
[Fe(TPP)(NO)][b]	406 (4.97)	475 (sh)	538 (4.00)		604 (3.45)	36
[Fe(TpivPP)(NO)][c]	407 (5.15)	477 (sh) (4.35)	539 (4.12)		607 (3.62)	25
[Fe(TMP)(NO)][d]	408 (4.96)	477 (sh)	539 (3.04)		611 (3.84)	37
[Fe(TPP)(CO)][e]	419		537	570	~610	38
[Fe(TpivPP)(NO_2)]$^-$ [c]	433 (sh) (4.94)	444 (5.12)	543 (sh) (3.89)	567 (4.02)	608 (3.59)	20, 22
Six-Coordinate Iron(II) Nitro						
[Fe(TpivPP)(NO_2)(CO)]$^-$ [c]	414 (sh) (4.67)	434 (5.30)	546 (3.98)			tw[f]
[Fe(TpivPP)(NO_2)(*t*-BuNC)]$^-$ [c]		441 (5.52)	541 (4.20)	572 (3.45)		tw
[Fe(TpivPP)(NO_2)(NO)]$^-$ [c]		433 (5.17)	543 (4.14)			21
[Fe(TpivPP)(NO_2)(Py)]$^-$ [c]	413 (sh) (4.83)	430 (5.23)	533 (4.21)	560 (sh) (3.66)	653 (2.83)	22
[Fe(TpivPP)(NO_2)(PMS)]$^-$ [c]	418 (sh) (4.88)	432 (5.07)	537 (4.18)	558 (sh) (3.81)	653 (3.12)	22
Six-Coordinate Iron(II) Other						
[Fe(TPP)(1-MeIm)(NO)][b]	415 (5.26)	460 (4.26)	545 (3.99)	580 (sh) (3.78)	643 (3.05)	39
[Fe(TPP)(4-NMe_2Py)(NO)][d]	416		554	586		40
[Fe(TPP)(1-MeIm)(NO)][d]	416		543	583	641	40
[Fe(TPP)(4-MePip)(NO)][d]	417	463	554	591		40
[Fe(TPP)(1-VinIm)$_2$][d]	424 (5.22)		533 (4.24)	564 (3.67)		41
[Fe(TPP)(1-BzlIm)$_2$][d]	426 (5.23)		533 (4.24)	565 (3.63)		41
[Fe(TPP)(1-AcIm)$_2$][d]	422 (5.14)		533 (3.99)	563 (3.62)		41
[Fe(TPP)(1-MeIm)$_2$][d]	425 (5.09)		533 (4.26)	564 (3.75)		41
[Fe(TpivPP)(1-MeIm)$_2$][c]	430		536			42
[Fe(TpivPP)(1-MeIm)$_2$][e]	432 (5.36)		537 (4.32)	562 (sh)		43
[Fe(TpivPP)(Im)(HIm$^-$)]$^-$ [c]	442 (4.00)		544 (3.47)			44
[Fe(TPP)(1-MeIm)(CO)][e]	427 (5.50)		542 (3.95)			43
[Fe(TPP)(1-MeIm)(CO)][d]	422		544			45
[Fe(TpivPP)(1-MeIm)(CO)][c]	425		542			42
[Fe(TPP)($CO)_2$][e]	426		551	578		38
Iron(II) Thiolates						
[Fe(TpivPP)(SEt)]$^-$ [c]	421		533	575	625	46
[Fe(TpivPP)(SEt)(CO)]$^-$ [c]	392, 467		565	612		46
[Fe(TpivPP)(SPh)]$^-$ [c]	421		536	575	625	46
[Fe(TpivPP)(SPh)(CO)]$^-$ [c]	403, 464		555	605		46
Six-Coordinate Iron(III) Nitro						
[Fe(TpivPP)($NO_2)_2$]$^-$ [c]	364 (sh)	426 (5.11)	464 (sh)	553 (4.15)		23
[Fe(TpivPP)(NO_2)(Py)][c]		422 (5.26) 459 (sh)	459 (sh)	550 (4.11)		24
[Fe(TPP)(NO_2)(NO)][b]		433 (5.34)	510 (sh) (3.70)	545 (4.20)	577 (sh) (3.70)	47
[Fe(Tp-OCH_3PP)(NO_2)(NO)][c]		437		549	586	26
[Fe(TpivPP)(NO_2)(NO)][e]		433		543	581	26

[a] All spectra were taken at 25 °C. [b] Chloroform solution. [c] Chlorobenzene solution. [d] Dichloromethane solution. [e] Toluene solution. [f] This work.

(Porph)$(L)_2$] species, there is a slight blue shift of the Soret maximum (Table 2). Similarly, when NO replaces a neutral N-donor ligand to give [Fe(TPP)(NO)(L)], the Soret band is also blue shifted compared to [Fe(TPP)$(L)_2$]. However, when the negatively charged nitrite ligand replaces a neutral N-donor ligand as in [Fe(TpivPP)(NO_2)(L)]$^-$, the Soret band is red shifted relative to the [Fe(Porph)$(L)_2$] species. The effect of the addition of an anionic ligand can also be seen upon comparison of [Fe(Porph)$(L)_2$] to [Fe(TpivPP)(Im$^-$)(HIm)]$^-$.[44] Again, a large red shift (~10 nm) of the Soret is seen. A red shift is also seen when comparing [Fe(TPP)(NO)(L)] to [Fe(TpivPP)(NO_2)(NO)]$^-$ where there is a replacement of a neutral N-donor ligand with the negatively charged nitrite ligand.

The addition of either of two well-known π-bonding ligands (CO or *tert*-butyl isocyanide) to the five-coordinate nitrite species, [Fe(TpivPP)(NO_2)]$^-$, lead to the new six-coordinate mixed-ligand species [Fe(TpivPP)(NO_2)(CO)]$^-$ or [Fe(TpivPP)(NO_2)(*t*-BuNC)]$^-$. The electronic spectra for these two species are given in Figure 6 along with that for [Fe(TpivPP)(NO_2)]$^-$. Clearly the spectra are different from the five-coordinate precursor and indicate that the new six-coordinate species persist in solution. The Soret bands have blue-shifted by as much as 10 nm for [Fe(TpivPP)(NO_2)(CO)]$^-$, and the visible bands have also blue-shifted by more than 20 nm upon coordination of the sixth ligand.

In addition, the spectrum of [Fe(TpivPP)(NO_2)(CO)]$^-$ has the characteristically sharp Soret band seen in other carbon monoxide porphyrinate complexes.[48−50] However, the Soret maximum is red-shifted (~10 nm) compared to CO com-

(36) Scheidt, W. R.; Frisse, M. E. *J. Am. Chem. Soc.* **1975**, *97*, 17.
(37) Mu, X. H.; Kadish, K. M. *Inorg. Chem.* **1988**, *27*, 4720.
(38) Wayland, B. B.; Mehne, L. F.; Swartz, J. *J. Am. Chem. Soc.* **1978**, *100*, 2379.
(39) Scheidt, W. R.; Piciulo, P. L. *J. Am. Chem. Soc.* **1976**, *98*, 1913.
(40) Wyllie, G. R. A.; Schulz, C. E.; Scheidt, W. R. *Inorg. Chem.* **2003**, *42*, 5722.
(41) Safo, M. K.; Scheidt, W. R.; Gupta, G. P. *Inorg. Chem.* **1990**, *29*, 626.
(42) Ellison, M. K.; Scheidt, W. R. Unpublished results.
(43) Collman, J. P.; Brauman, J. I.; Doxsee, K. M.; Halbert, T. R.; Bunnenberg, E.; Linder, R. E.; LaMar, G. N.; Del Guadio, J.; Lang, G.; Spartalian, K. *J. Am. Chem. Soc.* **1980**, *102*, 4182.
(44) Mandon, D.; Ott-Woelfel, F.; Fisher, J.; Weiss, R.; Bill, E.; Trautwein, A. X. *Inorg. Chem.* **1990**, *29*, 2442.
(45) Roth, A.; Scheidt, W. R. Unpublished results.

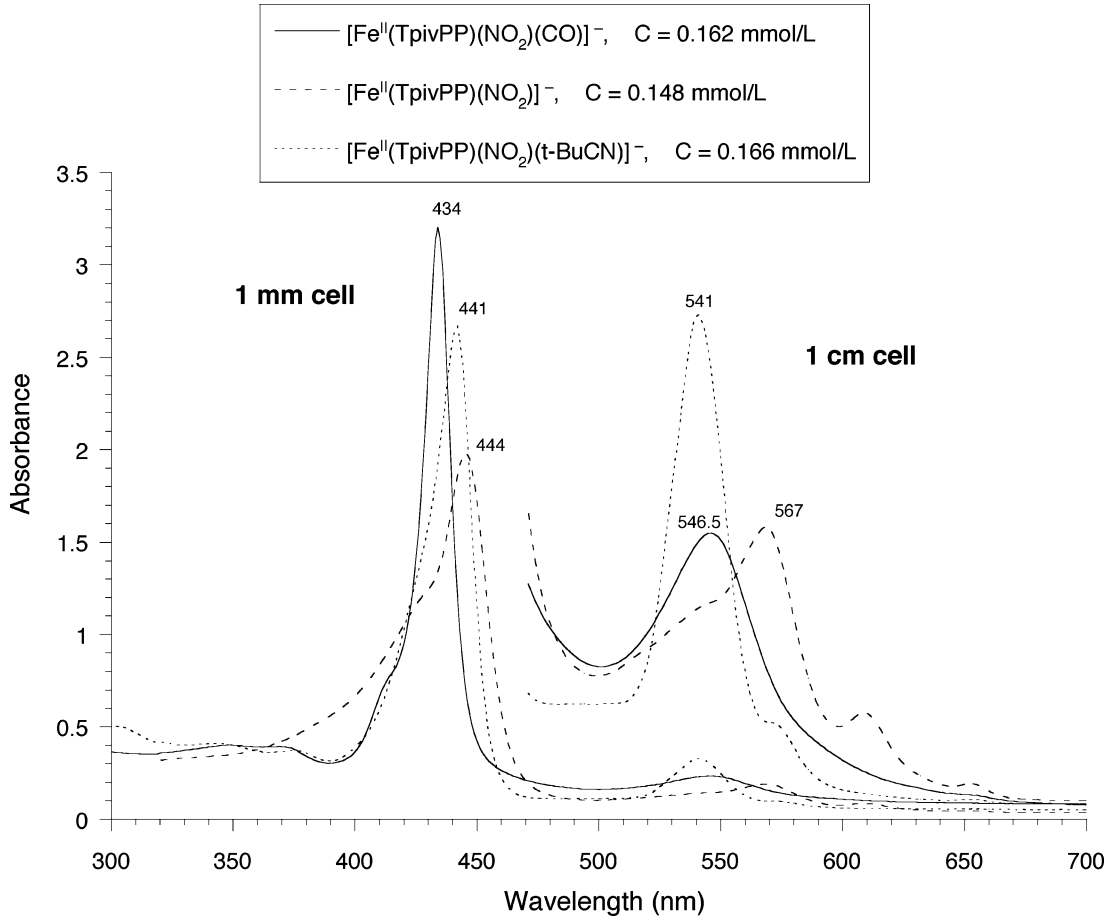

Figure 6. UV−vis spectra of $[Fe(TpivPP)(NO_2)]^-$, $[Fe(TpivPP)(NO_2)(CO)]^-$, and $[Fe(TpivPP)(NO_2)(t\text{-}BuNC)]^-$ taken under argon in chlorobenzene.

plexes with neutral ligands trans to CO ([Fe(Porph)(L)(CO)]) and to the bis(carbonyl) species $[Fe(TPP)(CO)_2]$. The effect of the negatively charged nitrite ligand is to shift the Soret maximum to the red as previously observed. Indeed, the wavelength maxima for $[Fe(TpivPP)(NO_2)(CO)]^-$ are remarkably similar to all of the other six-coordinate iron(II) *nitro* species given in Table 2. Not surprisingly, the electronic spectrum of $[Fe(TpivPP)(NO_2)(CO)]^-$ has characteristics of both six-coordinate iron(II) carbonyl and iron(II) nitro porphyrinates.

Mössbauer and structural studies revealed the exceptional π-accepting ability of nitrite in five-coordinate $[Fe(TpivPP)(NO_2)]^-$.[20] The axial $Fe-N(NO_2)$ bond is found to be very short at 1.849(6) Å, and the iron out-of-plane displacement at 0.18 Å is much smaller than the iron displacements found in high-spin iron(II) species. Mössbauer spectra obtained in a strong applied magnetic field (8 T) confirmed that the presence of a single nitrite ligand is sufficient to render $[Fe(TpivPP)(NO_2)]^-$ a low-spin complex.[20,51]

However, the nature of the π-accepting ability of nitrite is modulated by the presence of a sixth ligand. The changing π-bonding nature of nitrite was seen in the six-coordinate derivatives $[Fe(TpivPP)(NO_2)(PMS)]^-$ and $[Fe(TpivPP)(NO_2)(Py)]^-$.[22] The addition of the neutral ligand pentamethylene sulfide or pyridine to $[Fe(TpivPP)(NO_2)]^-$ diminished the π-bond to nitrite as evinced by the considerable increase (~0.1 Å on average) in the $Fe-N(NO_2)$ bond lengths in the new six-coordinate complexes.[56] The Mössbauer data shows a significant decrease in quadrupole splitting upon coordination of PMS or Py to the five-coordinate nitrite species. This large change results from a decreased rhombicity of the d_{xz} and d_{yz} orbitals that is attributed to a diminished π-bond between nitrite and iron(II) in the six-coordinate species.

We were also able to synthesize six-coordinate species with the two very good π-acceptor ligands NO and nitrite trans to each other. The two crystalline forms of $[Fe(TpivPP)(NO_2)(NO)]^-$[21] differ in that the two axial ligand planes

(46) Schappacher, M. Ph.D. Thesis, Université de Strasbourg, Strasbourg, France, 1982.
(47) Yoshimura, T. *Inorg. Chim. Acta* **1984**, *83*, 17.
(48) Stolzenberg, A. M.; Strauss, S. H.; Holm, R. H. *J. Am. Chem. Soc.* **1981**, *103*, 4763.
(49) Rougee, M.; Brault, D. *Biochemistry* **1975**, *14*, 4100.
(50) Wang, C.-M.; Brinigar, W. S. *Biochemistry* **1979**, *18*, 4960.
(51) All other five-coordinate iron(II) porphyrinates with a single anionic axial ligand are high spin. Some examples include the anions ethanethiolate,[14,52] chloride,[53] tetrafluorobenzenethiolate,[53] phenoxide,[54] 2-methylimidazolate,[44] and acetate.[55]
(52) Schappacher, M.; Ricard, L.; Fischer, J.; Weiss, R.; Montiel-Montoya, R.; Bill, E.; Trautwein, A. X. *Inorg. Chem.* **1989**, *28*, 4639.
(53) Schappacher, M.; Ricard, L.; Weiss, R.; Montiel-Montoya, R.; Gonser, U.; Bill, E.; Trautwein, A. X. *Inorg. Chim. Acta* **1983**, *78*, L9.
(54) Nasri, H.; Fischer, J.; Weiss, R.; Bill, E.; Trautwein, A. X. *J. Am. Chem. Soc.* **1987**, *109*, 2549.
(55) Bominaar, E. L.; Ding, X.; Gismelseed, A.; Bill, E.; Winkler, H.; Trautwein, A. X.; Nasri, H.; Fischer, J.; Weiss, R. *Inorg. Chem.* **1992**, *31*, 1845.
(56) The large change in $Fe-N(NO)_2$ bond length is not merely a result of change in coordination number. See ref 22 for a detailed discussion.

Table 3. Bond Distances (Å) for (Nitro)iron Porphyrin Derivatives

	$Fe-N_p$	$Fe-N_{NO_2}$	Fe−L	ref
Iron(II) Complexes				
$[Fe(TpivPP)(NO_2)(CO)]^-$ (**1**)	1.992(7)	2.006(4)	1.782(4)	tw[a]
$[Fe(TpivPP)(NO_2)(CO)]^-$ (**2**)	1.997(6)	2.009(4)	1.789(5)	tw
$[Fe(TpivPP)(NO_2)]^-$	1.970(4)	1.849(6)		20, 22
$[Fe(TpivPP)(NO_2)(PMS)]^-$	1.990(6)	1.937(3)	2.380(2)	22
$[Fe(TpivPP)(NO_2)(Py)]^-$	1.990(15)	1.951(5)	2.032(5)	22
$[Fe(TpivPP)(NO_2)(NO)]^-$ [b]	1.988(6)	2.086(8)	1.792(8)	21
$[Fe(TpivPP)(NO_2)(NO)]^-$ [c]	1.986(6)	2.060(7)	1.840(6)	21
Iron(III) Complexes				
$[Fe(TpivPP)(NO_2)(HIm)]$	1.974(2)	1.949(10)	2.037(10)	24
$[Fe(TpivPP)(NO_2)(Py)]$	1.985(3)	1.960(5)	2.093(5)	24
$[Fe(TpivPP)(NO_2)_2]^-$	1.992(1)	1.970(5)	2.001(6)	23
$[Fe(TpivPP)(NO_2)(SC_6HF_4)]^-$	1.980(7)	1.990(7)	2.277(2)	25
$[Fe(TpivPP)(NO_2)(NO)]$[d]	2.000(5)	2.002(2)	1.668(2)	26
$[Fe(TpivPP)(NO_2)(NO)]$[e]	1.996(4)	1.998(2)	1.671(2)	26

[a] This work. [b] ⊥ form. [c] || form. [d] *C*2/*c* form. [e] $P2_1/n$ form.

(FeNO and NO_2) have either parallel or perpendicular orientations with respect to each other. Surprisingly, the Mössbauer data show that the form with the perpendicular ligand planes maximizes the π-bonding of both nitrite and NO compared to the parallel form where the increased competition for π-density leads to strong π-bonding by NO alone.

Further investigations of the unusual nature of nitrite as an axial ligand led us to add two well-known π-bonding ligands (CO or *tert*-butyl isocyanide) to the five-coordinate nitrite species. We were able to synthesize and crystallize two new six-coordinate mixed-ligand species, $[Fe(TpivPP)(NO_2)(CO)]^-$ and $[Fe(TpivPP)(NO_2)(t\text{-BuNC})]^-$. The X-ray structures of $[Fe(TpivPP)(NO_2)(CO)]^-$ and $[Fe(TpivPP)(NO_2)(t\text{-BuNC})]^-$ unambiguously confirm the ligation at iron. The coordination group geometry can also yield information about the effect of an added trans ligand by comparison to previously characterized nitro and carbonyl porphyrin complexes. This discussion will be limited to the structure of $[Fe(TpivPP)(NO_2)(CO)]^-$ since the structure of $[Fe(TpivPP)(NO_2)(t\text{-BuNC})]^-$ did not yield adequately quantitative geometric parameters.

The molecular structures of the two independent anions in the asymmetric unit of $[Fe(TpivPP)(NO_2)(CO)]^-$ are shown in Figures 1 and 2. Tables 3 and 4 give selected bond lengths and angles for both anions as well as those of structurally characterized (nitro)iron and (carbonyl)iron(II) porphyrin derivatives. The nitrite ligand is bound within the picket fence porphyrin pocket in both anions, which is clearly the preferred binding site for an anionic ligand.[57] The nitrite ligand is N-bound as is nearly always the case for iron porphyrinates but not the ruthenium or osmium analogues. In both anions, the nitro ligand plane nearly bisects an N_p-Fe-N_p angle as expected. The orientation of the nitrite ligands with respect to the porphyrin cores are illustrated in Figures 3 and 4, which are views of anion **1** and anion **2**, respectively, from the picket side of the porphyrin plane. As evident from Figure 3, this ∼45° angle places the oxygen atoms of the nitrite ligand in line with the pivalamide arms. In the case of anion **1** the oxygen atoms then sit nestled between two methyl groups of the *tert*-butyl groups of the opposite pivalamide arms. This methyl group orientation is the most common arrangement for picket fence nitro derivatives. The rotational disorder of the nitro ligand and two adjacent *tert*-butyl groups in anion **2** is shown in Figure 4. This disorder makes it impossible to describe the orientation of the nitro ligand with respect to the methyl groups with certainty. However, the occupancy of the nitrite ligand oxygen atoms O(4a) and O(5a) is 54% and this occupancy nearly coincides with the methyl groups C(64), C(65), and C(66) which have a refined occupancy of 56%.

The average equatorial $Fe-N_p$ bond length for $[Fe(TpivPP)(NO_2)(CO)]^-$ (**1**) is 1.992(7) Å and for $[Fe(TpivPP)(NO_2)(CO)]^-$ (**2**) is 1.997(6) Å. These average bond lengths are the same as those found for the six-coordinate nitro species $[Fe(TpivPP)(NO_2)(PMS)]^-$,[22] $[Fe(TpivPP)(NO_2)(Py)]^-$,[22] and $[Fe(TpivPP)(NO_2)(NO)]^-$.[21] The average distance for these six-coordinate species is 0.02 Å longer than in the five-coordinate nitro species, $[Fe(TpivPP)(NO_2)]^-$. It is also slightly shorter (by 0.01 Å) than the $Fe-N_p$ bond length average of other CO complexes (confer Table 3).

The iron−axial ligand bond lengths are sensitive to bonding changes, and the largest structural changes occur upon coordination of a sixth ligand. The $Fe-N(NO_2)$ bond lengths for $[Fe(TpivPP)(NO_2)(CO)]^-$ (**1**) and $[Fe(TpivPP)(NO_2)(CO)]^-$ (**2**) are 2.006(4) and 2.009(4) Å, respectively. These are 0.16 Å longer than the $Fe-N(NO_2)$ bond length of $[Fe(TpivPP)(NO_2)]^-$. This substantial increase must reflect a dramatic change in the bonding between iron and nitrite upon coordination of CO. The $Fe-N(NO_2)$ bond lengths for both anions are also longer (by ∼0.06 Å) than in the six-coordinate nitro species with neutral ligands trans to nitrite $[Fe(TpivPP)(NO_2)(PMS)]^-$ and $[Fe(TpivPP)(NO_2)(Py)]^-$.[22] We interpret these increases in $Fe-N(NO_2)$ bond lengths in the two forms of $[Fe(TpivPP)(NO_2)(CO)]^-$ as a dramatic decrease in the π-bonding between iron and nitrite due to the presence of the strong π-acceptor ligand CO trans to nitrite. Nitrite appears again to vary its π-bonding ability depending on the other ligands at iron. This variable bonding behavior of nitrite is in distinct contrast to a similarly strong π-acceptor ligand NO, which we have termed an obligatory π-bonder since its π-bonding capability is nearly independent of the coordination number and ligation at iron.

So, is the bonding between iron and CO affected by the trans nitrite ligand? This is a more difficult question to answer since there is a limited variety of (carbon monoxide)-iron(II) porphyrinate complexes with which to compare. A five-coordinate example has not yet been structurally characterized, and the six-coordinate examples are mostly limited to those with neutral nitrogen donor ligands trans to CO. The Fe−C(CO) bond lengths in $[Fe(TpivPP)(NO_2)(CO)]^-$ (**1**) and $[Fe(TpivPP)(NO_2)(CO)]^-$ (**2**) are 1.782(4) and 1.789(5) Å, respectively. These bond lengths are within the range observed or possible slightly longer than those seen for all

(57) The only exceptions are two isomorphous forms of $[Fe(TpivPP)(NO_2)(NO)]$ for which the synthesis was designed to place the anionic ligand on the open face. The actual result was disorder of the axial ligands with a 57% occupancy of a nitro group on the open face of the picket fence porphyrin and a linear nitrosyl group inside the pocket. In the second case there was a 26% occupancy of the nitro out of the pocket.[26]

Table 4. Bond Parameters for (Carbon monoxide)iron Porphyrin Derivatives

complex	Fe−N_p[a]	Fe−C(CO)[a]	Fe−L[a]	Fe−C−O[b]	C−O[a]	ref
[Fe(TpivPP)(NO_2)(CO)]$^-$ (**1**)	1.992(7)	1.782(4)	2.006(4)	175.5(4)	1.150(5)	tw[c]
[Fe(TpivPP)(NO_2)(CO)]$^-$ (**2**)	1.997(6)	1.789(5)	2.009(4)	177.5(4)	1.140(5)	tw
[Fe(TPP)(Py)(CO)]	2.02(3)	1.77(2)	2.10(1)	179(2)	1.12(2)	10
[Fe(Deut)(THF)(CO)]	1.98(3)	1.706(5)	2.127(4)	178.3(14)	1.144(5)	13
[Fe(TPP)(SEt)(CO)]	1.993(4)	1.78(1)	2.352(2)	NR	1.17(1)	14
[Fe(TPP)(1-MeIm)(CO)]	1.999(7)	1.756(2)	2.059(1)	178.91(17)	1.147(2)	*d*
	2.003(5)	1.793(3)	2.071(2)	179.3(3)	1.061(3)	11
[Fe(OEP)(1-MeIm)(CO)]	2.000(3)	1.744(5)	2.077(3)	175.1(4)	1.158(5)	12
[Fe(TPpiv_2C_{12}P)(1-MeIm)(CO)]	1.999(3)	1.728(6)	2.062(5)	∼180	1.149(6)	15
[Fe(β-PocpivP)(1,2-Me_2Im)(CO)]	1.973(8)	1.768(7)	2.079(5)	172.5(6)	1.148(7)	16
[Fe(C_2-Cap)(1-MeIm)(CO)]	1.990(7)	1.742(7)	2.043(6)	172.9(6)	1.161(8)	17
	1.988(13)	1.748(7)	2.041(5)	175.9(6)	1.158(8)	17
[Fe(OC_3OPor)(1-MeIm)(CO)]	1.996(12)	1.748(7)	2.027(5)	173.9(9)	1.171(8)	18
[Fe(OC_3OPor)(1,2-Me_2Im)(CO)]	2.00(2)	1.713(8)	2.102(6)	180[e]	1.161(10)	18
[Fe(C_3-Cap)(1-MeIm)(CO)]	1.99(2)	1.800(13)	2.046(10)	178.0(13)	1.107(13)	19

[a] Value in Å. [b] Value in deg. [c] This work. [d] An, J.; Beatty, A.; Scheidt, W. R. Unpublished result. [e] Required by symmetry.

[Fe(Porph)(L)(CO)] species (Table 4). The Fe−C−O angles for the two anions are essentially linear and again within the normal range. From Figure 5 we see that the iron atom is displaced toward the CO ligand in both of the anions. The core nitrogen atoms are also domed toward CO. These two features suggest that CO is the more dominant of the two axial ligands. It thus appears from the structural data that the CO is clearly the more dominant of the two ligands and nitrite has varied its π-acidity to suit the bonding situation. Any changes in bonding should also be manifested in other physical properties. Accordingly, the bonding nature of nitrite and CO in [Fe(TpivPP)(NO_2)(CO)]$^-$ was also examined with infrared and Mössbauer spectroscopies.

The vibrational spectroscopy of CO complexes shows high sensitivity to bonding changes. Fe−CO bonding is regarded as being dominated by back-donation from the iron d_π electrons to the π^* orbitals of CO. The Fe−C−O bond is essentially linear, and there is a negative correlation between the Fe−C(CO) stretch and the C−O stretch. That is, ν(Fe−C(CO)) increases as ν(C−O) decreases. The stretching frequency of CO should thus reflect changes in the electronic environment at iron. If we compare ν(CO) for [Fe(TpivPP)(NO_2)(CO)]$^-$ (1974 cm^{-1}, KBr) to other six-coordinate species of the general formula [Fe(Porph)(L)(CO)], we see a slight increase in energy. For [Fe(TPP)(1-MeIm)(CO)] ν(CO) is 1969 cm^{-1} in CD_2Cl_2, and for [Fe(OEP)(1-MeIm)(CO)] ν(CO) is 1965 cm^{-1} in CH_2Cl_2. Unfortunately, a comparison to a five-coordinate species is not available. This slight increase in ν(CO) compared to those species with a neutral nitrogen-donor ligand trans to CO means there is only slightly less π-back-bonding from iron to CO. The implication is that nitrite has very little π-bonding influence in agreement with the structural findings.

An analysis of the metal−ligand bonding interaction can be made with Mössbauer spectroscopy, which is quite sensitive to changes in the electronic environment at iron. An important study by Trautwein and co-workers[62] demonstrates the effect of axial ligand bonding properties on the quadrupole splitting for several d^6 pseudooctahedral complexes. They found that the ΔE_Q values for iron(II) porphyrinates of the general formula [Fe(Porph)$(L)_2$] where L is an imidazole or pyridine are greater than 0.9 mm/s and less than 1.7 mm/s. This range of values also agrees with solid-state measurements on similar species (confer Table 5). As these authors predict by the Townes−Dailey approximation,[74] replacing the imidazoles or pyridines (which are generally good σ-donors) with good π-acceptors such as trimethylphosphine or CO causes the quadrupole splitting to decrease. Replacing two σ-donors with two π-acceptors decreases ΔE_Q even more. On the basis of this analysis, we should expect that [Fe(TpivPP)(NO_2)(CO)]$^-$ will have a smaller ΔE_Q value than [Fe(TpivPP)(NO_2)(Py)]$^-$ and [Fe(TpivPP)(NO_2)(PMS)]$^-$.

However, the effect of nitrite on ΔE_Q is hard to predict since its variable σ-donor and π-acceptor bonding properties have competing effects on ΔE_Q. As discussed earlier, the two crystalline forms of [Fe(TpivPP)(NO_2)(NO)]$^-$,[21] which differ in the orientation of the axial ligand planes, have different ΔE_Q values.[75] If we compare these values to

(58) Safo, M. K.; Nesset, M. J. M.; Walker, F. A.; Debrunner, P. G.; Scheidt, W. R. *J. Am. Chem. Soc.* **1997**, *119*, 9438.
(59) Kobayashi, H.; Maeda, Y.; Yanagawa, Y. *Bull. Chem. Soc. Jpn.* **1970**, *43*, 2342.
(60) Dolphin, D.; Sams, J. R.; Tsin, T. B.; Wong, K. L. *J. Am. Chem. Soc.* **1976**, *98*, 6970.
(61) Collman, J. P.; Hoard, J. L.; Kim, N.; Lang, G.; Reed, C. A. *J. Am. Chem. Soc.* **1975**, *97*, 2676.
(62) Polam, J. R.; Wright, J. L.; Christensen, K. A.; Walker, F. A.; Flint, H.; Winkler, H.; Grodzicki, M.; Trautwein, A. X. *J. Am. Chem. Soc.* **1996**, *118*, 5272.
(63) Havlin, R. H.; Godbout, N.; Salzmann, R.; Wojdelski, M.; Arnold, W.; Schulz, C. E.; Oldfield, E. *J. Am. Chem. Soc.* **1998**, *120*, 3144.
(64) Conner, W. M.; Straub, D. K. *Inorg. Chem.* **1976**, *15*, 2289.
(65) Maeda, Y.; Harami, T.; Morita, Y.; Trautwein, A. X.; Gonser, U. *J. Chem. Phys.* **1981**, *75*, 36.
(66) Cao, C.; Dahal, S.; Shang, M.; Beatty, A. M.; Hibbs, W,; Schulz, C. E.; Scheidt, W. R. *Inorg. Chem.* **2003**, *42*, 5202.
(67) Bohle, D. S.; Debrunner, P.; Fitzgerald, J.; Hansert, B.; Hung, C.-H.; Thompson, A. J. *J. Chem. Soc., Chem. Commun.* **1997**, 91.
(68) Wyllie, G. R. A.; Scheidt, W. R. *Inorg. Chem.* **2003**, *42*, 4259.
(69) Ellison, M. K.; Schulz, C. E.; Scheidt, W. R. *Inorg. Chem.* **2000**, *39*, 5102.
(70) Ellison, M. K.; Schulz, C. E.; Scheidt, W. R. *J. Am. Chem. Soc.* **2002**, *124*, 13833.
(71) Schünemann, V.; Benda, R.; Trautwein, A. X.; Walker, F. A. *Isr. J. Chem.* **2000**, *40*, 9.
(72) Settin, M. F.; Fanning, J. C. *Inorg. Chem.* **1988**, *27*, 1431.
(73) Richter-Addo, G. B.; Wheeler, R. A.; Hixson, C. A.; Chen, L.; Khan, M. A.; Ellison, M. K.; Schulz, C. E.; Scheidt, W. R. *J. Am. Chem. Soc.* **2001**, *123*, 6314.
(74) Paulsen, H.; Krockel, M.; Grodzicki, M.; Bill, E.; Trautwein, A. X.; Leigh, G. J.; Silver, J. *Inorg. Chem.* **1995**, *34*, 6244.

Table 5. Solid-State Mössbauer Parameters for $[Fe(TpivPP)(NO_2)(CO)]^-$ and Related Complexes

	ΔE_Q, mm/s	δ_{Fe}, mm/s	*T*, K	ref
[Fe(TpivPP)(NO_2)(CO)]	0.32	0.18	293	tw[a]
	0.28	0.28	15	tw
Iron(II) Complexes				
[Fe(TMP)($Py)_2$]	1.24	0.45	4.2	58
[Fe(TPP)($Py)_2$]	1.15	0.40	77	59
[Fe(OEP)($Py)_2$]	1.13	0.46	4.2	60
[Fe(TPP)(1-VinIm)$_2$]	1.00	0.43	4.2	41
[Fe(TPP)($Pip)_2$]	1.44	0.51	4.2	61
[Fe(TpivPP)(1-MeIm)$_2$]	1.02	0.46	4.2	61
[Fe(TMP)(1-MeIm)$_2$][b]	1.11	0.45	77	62
[Fe(OEP)(1-MeIm)$_2$][b]	0.96	0.46	77	62
[Fe(TMP)(PMe_3)(1-MeIm)][b]	0.75	0.38	77	62
[Fe(TMP)($PMe_3)_2$][b]	0.47	0.36	77	62
[Fe(OEP)($PMe_3)_2$][b]	0.35	0.36	77	62
Iron(II) CO and CS Complexes				
[Fe(TPP)(1-MeIm)(CO)]	0.35	0.20	293	63
[Fe(TPP)(Py)(CO)]	0.57	0.28	293	63
[Fe(T*p*-OCH_3PP)(Py)(CO)]	0.49	0.19	298	64
[Fe(T*p*-OCH_3PP)(HIm)(CO)]	0.36	0.18	298	64
[Fe(TpivPP)(1-MeIm)(CO)]	0.27	0.27	4.2	30
MbCO	0.35	0.27	4.2	65
[Fe(OEP)(4-CNPy)(CS)]	0.80	0.19	4.2	66
[Fe(OEP)(Py)(CS)]	0.57	0.15	4.2	66
[Fe(OEP)(Pip)(CS)]	0.65	0.19	4.2	66
[Fe(OEP)(4-NMe_2Py)(CS)]	0.44	0.19	4.2	66
[Fe(OEP)(1-MeIm)(CS)]	0.42	0.14	4.2	66
Iron(II) Nitro Complexes				
[Fe(TpivPP)(NO_2)]	2.28	0.41	4.2	22
[Fe(TpivPP)(NO_2)(PMS)]	1.18	0.42	4.2	22
[Fe(TpivPP)(NO_2)(Py)]	0.93	0.41	4.2	22
{FeNO}[7] Complexes				
$[Fe(TpivPP)(NO_2)(NO)]^-$ [c]	1.78	0.22	200	21
$[Fe(TpivPP)(NO_2)(NO)]^-$ [d]	1.20	0.35	4.2	21
[Fe(TPP)(NO)]	1.24	0.35	4.2	21
[Fe(OEP)(NO)]	1.26	0.35	100	67
[Fe(Deut)(NO)]	1.47	0.39	4.2	68
[Fe(TPP)(1-MeIm)(NO)]	0.73	0.35	4.2	40
[Fe(TPP)(4-MePip)(NO)]	0.91	0.37	4.2	40
Iron(III) Nitro Complexes				
[Fe(TpivPP)($NO_2)_2$]	2.1	0.25	4.2	24
[Fe(TpivPP)(NO_2)(Py)]	2.2	0.26	4.2	24
[Fe(TpivPP)(NO_2)(SC_6HF_4)]	2.12	0.22	293	25
	2.30	0.28	4.2	25
{FeNO}[6] Complexes				
$[Fe(OEP)(Iz)(NO)]^+$	1.99	−0.07	293	69
	1.92	0.02	4.2	69
$[Fe(OEP)(2\text{-}MeHIm)(NO)]^+$	1.88	0.05	4.2	70
$[Fe(OEP)(1\text{-}MeIm)(NO)]^+$ [b]	1.64	0.02	4.2	71
[Fe(OEP)(NO)]ClO_4	1.55	0.13	293	69
	1.64	0.20	4.2	69
[Fe(T*p*-OCH_3PP)(NO_2)(NO)]	1.43	0.04	293	26
[Fe(TpivPP)(NO_2)(NO)]	1.48	0.01	293	26
	1.43	0.09	4.2	26
[Fe(TPP)(NO_2)(NO)]	1.37	0.02	293	26
	1.36	0.13	4.2	26
	1.36	0.13	77	72
[Fe(OEP)(C_6H_4-*p*-F)(NO)]	0.56	0.05	293	73
	0.57	0.14	4.2	73

[a] This work. [b] In dimethylacetamide solution. [c] ⊥ form. [d] || form.

[Fe(Porph)(NO)], we see the effect of nitrite on the bonding is negligible (two ligand planes parallel) or more significant (two ligand planes perpendicular). Thus, nitrite was termed a variable π-bonder. We also see the diminished importance of nitrite on the bonding in $[Fe(TpivPP)(NO_2)(CO)]^-$ where a quadrupole splitting value of 0.28 mm/s at 15 K is observed. The quadrupole splitting is within the range seen for carbonyl complexes with neutral nitrogen donor ligands trans to CO ([Fe(Porph)(L)(CO)] and MbCO; Table 5). Thus, the decreased importance of the nitrite ligand on the bonding is clearly manifested in the Mössbauer parameters.

In addition, we have recently shown the effect of the π-accepting ligand NO on isomer shifts for a series of {FeNO}[6] complexes.[69] These formally iron(III) species have very small isomer shifts indicating high formal charge at iron compared to other iron(III) complexes of the general formula $[Fe(Porph)(L)_2]$. There is also a decrease in the isomer shift when iron(II) porphyrinates with a carbonyl ligand ([Fe(Porph)(L)(CO)]) or iron(II) nitrosyl complexes are compared with typical low-spin $[Fe(Porph)(L)_2]$ complexes. Small isomer shift values are indicative of strong π-donation from iron to its ligands (CO or NO). The temperature-dependent isomer shift for $[Fe(TpivPP)(NO_2)(CO)]^-$ is 0.18 mm/s at 293 K and 0.28 mm/s at 15 K. This unusually small isomer shift value for iron(II) complexes is within the range observed for other iron(II) *CO* porphyrinates and is consistent with our interpretation that the π-accepting carbonyl ligand dominates the bonding. Six-coordinate thiocarbonyl (CS) complexes (Table 5) also show such decreased isomer shifts. Neese and co-workers also show for a series of octahedral iron complexes that the isomer shift decreases with increasing π-accepting ability of the axial ligand.[76] A detailed DFT study also predicts small isomer shifts for species with strongly back-bonding ligands.[77]

Summary

Two new six-coordinate iron(II) mixed-ligand porphyrinates have been synthesized and characterized. The single-crystal structure determination of $[K(222)][Fe(TpivPP)(NO_2)(CO)]\cdot 1/2C_6H_5Cl$ clearly shows that the bonding parameters of the FeCO group are normal and virtually unaffected by the nitrite ligand trans to it. However, the Fe−$N(NO_2)$ bond is elongated compared to the five-coordinate nitrite species, strongly suggesting that the nitrite ligand has diminished π-bonding to accommodate six-coordination. Infrared and Mössbauer data confirm that in the competition between these two strong, π-accepting axial ligands CO dominates the bonding and nitrite has reduced π-bonding to fit the bonding situation. Thus, Mössbauer, structural studies, and vibrational spectra are all consistent in supporting our conclusion that CO is the much stronger π-bonded axial ligand. We see that there is a continuum of nitrite behavior as a π-bonding ligand. In $[Fe(TpivPP)(NO_2)]^-$, it is a very strong π-bonder but much weaker in this new CO complex. Nitrite is a moderate π-bonding ligand in the other six-coordinate complexes including the iron(III) bis(nitro) species, $[Fe^{II}(TpivPP)(NO_2)(L)]^-$ species, and the iron(II) nitro

(75) The quadrupole splittings (ΔE_Q) for the two geometric forms of $[Fe(TpivPP)(NO_2)(NO)]^-$ are significantly different. Although the Mössbauer spectra for the two forms were taken at two different temperatures, any temperature-dependent effect on ΔE_Q is unlikely to make the two values more equivalent.

(76) Li, M.; Bonnet, D.; Bill, E.; Neese, F.; Weyhermüller, T.; Blum, N.; Sellman, D.; Wieghardt, K. *Inorg. Chem.* **2002**, *41*, 3444.
(77) Neese, F. *Inorg. Chim. Acta* **2002**, *337*, 181.

nitrosyls. A study such as this on the subject of π-bonding is of great interest especially as it pertains to reactivity. Tuning of the π interaction between axial ligands and metalloporphyrin centers could be an important controller of reactivity and fuction.

Acknowledgment. We thank the National Institutes of Health for support of this research under Grant GM-38401. Funds for the purchase of the FAST area detector diffractometer were provided through NIH Grant RR-06709 to the University of Notre Dame.

Supporting Information Available: Tables S1−S6, giving complete crystallographic details, atomic coordinates, bond distances and angles, anisotropic temperature factors, and fixed hydrogen atom positions for [K(222)][Fe(TpivPP)(NO_2)(CO)]·1/2C_6H_5Cl, Figures of K(222) cations and complete labeled diagrams of the [Fe(TpivPP)(NO_2)(CO)]$^-$ anions (PDF) and an X-ray crystallographic file, in CIF format. This material is available free of charge via the Internet at http://pubs.acs.org.

IC035119Y